REPORT DOCUMENTATION PAGE

1. REPORT DATE *(DD-MM-YYYY)*	2. REPORT TYPE	3. DATES COVERED *(From - To)*
	Technical Papers	

4. TITLE AND SUBTITLE

5a. CONTRACT NUMBER

5b. GRANT NUMBER

5c. PROGRAM ELEMENT NUMBER

6. AUTHOR(S)

5d. PROJECT NUMBER

5e. TASK NUMBER

5f. WORK UNIT NUMBER

7. PERFORMING ORGANIZATION NAME(S) AND ADDRESS(ES)

Air Force Research Laboratory (AFMC)
AFRL/PRS
5 Pollux Drive
Edwards AFB CA 93524-7048

8. PERFORMING ORGANIZATION REPORT

9. SPONSORING / MONITORING AGENCY NAME(S) AND ADDRESS(ES)

Air Force Research Laboratory (AFMC)
AFRL/PRS
5 Pollux Drive
Edwards AFB CA 93524-7048

10. SPONSOR/MONITOR'S ACRONYM(S)

11. SPONSOR/MONITOR'S NUMBER(S)

12. DISTRIBUTION / AVAILABILITY STATEMENT

Approved for public release; distribution unlimited.

13. SUPPLEMENTARY NOTES

14. ABSTRACT

20020830 098

15. SUBJECT TERMS

16. SECURITY CLASSIFICATION OF:			17. LIMITATION OF ABSTRACT	18. NUMBER OF PAGES	19a. NAME OF RESPONSIBLE PERSON Leilani Richardson
a. REPORT	b. ABSTRACT	c. THIS PAGE	A		19b. TELEPHONE NUMBER *(include area code)* (661) 275-5015
Unclassified	Unclassified	Unclassified			

5 items enclosed

MEMORANDUM FOR PRS (In-House/Contractor Publication)

FROM: PROI (STINFO)   19 July 2002

SUBJECT: Authorization for Release of Technical Information, Control Number: **AFRL-PR-ED-TP-2002-188**
C.T. Liu (PRSM) and M. Tam (Aerospace), "Investigating the Effects of Pressure on the Near Tip
Behavior and Crack Growth in a Particulate Composite Material"

(55642)

Int'l Conf. Fracture & Damage Mechanics 2002   (Statement A)
(Maui, HI, 15-17 October 2002) (Deadline: 20 August 2002)

Investigating the Effects of Pressure on the Near Tip Behavior and Crack Growth in a Particulate Composite Material

C.T.Liu[1] & M. Tam[2]
[1] Propulsion Directorate, U.S. Air Force Research Laboratory,
U.S.A.
[2] The Aerospace Co. U.S.A.

Abstract

In this study, the effects of different loading conditions on the local behavior and crack growth in a particulate composite material were investigated. The material under investigation contains hard particles embedded in a rubbery matrix. Two loading conditions, constant strain rate and constant strain, and two confined pressures, ambient and 8697 KPa, were considered. The experimental data were analyzed and the results are discussed.

1 Introduction

In past years, a considerable amount of work has been done studying crack growth behavior in particulate composite materials under different loading conditions at ambient pressure [1-4]. The basic approach used in characterizing the crack growth behavior in the particulate composite materials is based on linear elastic or linear viscoelastic fracture mechanics. Experimental findings indicate that power law relationships exist between the crack growth rate, da/dt, and the Mode I stress intensity factor, K_I. These experimental findings support the theory developed by Knauss [5] and Schapery [6] in their studies of crack growth behavior in linear viscoelastic materials. It is known that classical fracture mechanics principles, especially linear elastic fracture mechanics, are well established for single-phase materials. Experimental data indicate that linear fracture mechanics theories are applied to particulate composite materials with varying degrees of success. However, relatively little effort has been made

to understand the crack growth behavior in such materials under confined pressure conditions.

In this study, pre-cracked specimens were used to study crack growth behavior in a particulate composite material, containing hard particles embedded in a rubbery matrix, under two different loading conditions, constant strain rate and constant strain, at ambient and 8697 KPa confined pressures. The effects of pressure on the local strain fields near the crack tip, the crack opening displacement, and the crack growth behavior in the material were investigated and the results are discussed.

2 The Experiments

In this study, specimens with a pre-cracked surface crack were used to determined the crack growth behavior in a particulate composite material subjected to two different loading histories, constant strain rate and constant strain, at ambient and 8697 KPa confined pressures. The geometry of the pre-cracked specimen is shown in Fig.1. Prior to conducting the tests, the specimen was loaded in the testing machine inside a pressure chamber. When the pressure inside the pressure chamber reached 8697 KPa, the specimen was straining at a constant strain rate of 5.8 cm/cm/min. For the constant strain rate loading condition, the specimen was stretched until it broke. For the constant strain loading condition, the specimen was stretched until a perdetermined strain level of 18% was reached. During the test, a high-speed camera was used to monitor the crack growth. In addition, the load and time were also recorded. These raw data were used to determine the stress, strain, crack length, and crack growth rate.

To determine the strain fields near the crack tip, a Large Deformation Image Correlation (LDDIC) program, developed by Gonzalez [7] and Vendroux et.al. [8] was used. The LDDIC program was developed by modifying a Digital Image Correlation (DIC) program developed by Sutton et.al.[9] for small deformations. The problem in applying DIC to compute strain fields in a large deformation process is the failure of convergence of the DIC algorithm if the strain is larger than 10%. To circumvent this problem, the LDDIC takes intermediate images (or steps) of the deformation between the undeformed and the deformed states of the deformation, and, then, computes the displacements and the displacement gradients for every step of the deformation. The intermediate results are combined to produce the displacements and displacement gradients for the global deformation.
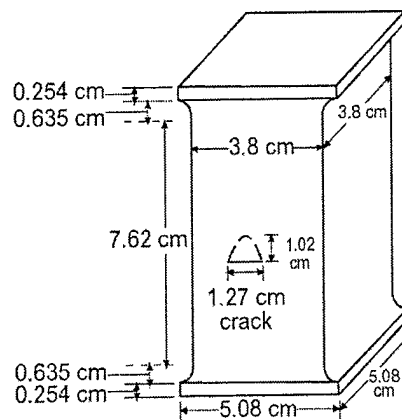
Figure 1 . Specimen geometry.

In order to check the accuracy of the digital image correlation technique, a specimen of homogeneous silicone rubber without a crack and coated with microscopic speckles was stretched sequentially and uniaxially to a maximum strain of 70% in a sequence of 12 deformation steps of 5.08% strain each. These strains were recorded (optically) with the aid of a microscope by keeping track of special marks (equal to prescribed strain). In addition, the digital image correlation program was used to compute the strain at a given deformation step. A comparison of the prescribed strain, obtained optically, and the computed strain, obtained by digital image correlation technique, revealed that a maximum deviation of 1% occurs at a strain of 40%. This precision is considered to be acceptable for experimental mechanics investigations.

3 Results and Discussion

It is well known that, on the microscopic scale, a highly filled polymeric material can be considered an inhomogeneous material. When these materials are stretched, the different sizes and distribution of filled particles, the different crosslink density of polymeric chains, and the variation in bond strength between the particles and the binder can produce highly nonhomogeneous local stress and strength fields. Depending on the magnitude of the local stress and the local strength, damage can develop in the material, especially near the crack tip region. The damage developed in the material may be in the form of microvoids or microcracks in the binder or dewetting between the binder and the filler particles. Damage growth in the material may occur as material tearing or as successive nucleation and coalescence of the microcracks. These damage processes are time dependent and they are the main factor responsible for the time sensitivity of strength degradation as well as the fracture behavior of the

material. Therefore, obtaining a better understanding of crack growth behavior requires detailed knowledge of damage mechanisms in the crack tip region.

When cracks occur, whether resulting from the manufacturing process or from service loads, the stresses near the crack tip will be redistributed according to nonlinear material behavior. Depending on the magnitude of the local stresses and the local strength, various defects, microvoids or microcracks, can develop in the crack tip region. And, depending on the severity of these defects, crack growth behavior can be significantly affected. Therefore, to obtain a fundamental understanding of crack growth behavior in particulate composite materials, the effect of defects on local fracture behavior near the crack tip needs to be determined.

Experimental results indicate that crack tip blunting takes place both before and after crack growth. The material at the tip of the crack suffers very large elongation and is nearly straight. The highly strained or damage zone extends ahead of the crack tip, appearing as an equilateral triangle with the crack tip as its base. This damage zone is known as the failure process zone, which is a key parameter in viscoelastic fracture mechanics. When the local strain reaches a critical value, small voids are generated in the failure process zone. Due to the random nature of the microstructure, the first void is not restricted to the surface where the maximum normal strain occurs. Since the tendency of the filler particle to separate from the binder under a triaxial loading condition is high, it is expected that voids, or a damage zone, will also be generated in the specimen's interior. Consequently, there are a large number of strands, essentially made of binder material, which separate the voids that form inside the failure process zone. Under this condition, the transverse constant is minimized. As the applied strain increases with time, material fracture occurs at the blunted end of the crack tip. This will always be the location of the maximum local strain. The failure of the material between the void and the crack tip causes the crack to grow into the failure process zone. This kind of crack growth mechanism continues until the main crack tip reaches the front of the failure process zone. When this occurs, the crack tip resharpens temporarily.

The damage and crack growth mechanisms discussed in the above paragraphs are the basic mechanisms observed in this material under both ambient and 8697 KPa pressures. The effect of pressure is to suppress the damage and evolution processes.

Typical plots of stress-strain curves with and without surface crack tested under ambient and 8697 KPa confined pressures are shown in Figs. 2 and 3. From Figs. 2 and 3, it is seen that for the specimen without crack, the stiffness, maximum stress, maximum strain, and rupture strain increase significantly when the pressure is increased from ambient to 8697 KPa. However, for the cracked specimen, the 8697 KPa confined pressure has a large effect on the maximum stress and a small effect on the maximum strain. The rupture strain reduces

from 50% for the specimen without crack to 25% for the specimen with crack under 8697 KPa confined pressure. This implies that the failure of the cracked specimen is controlled by the growth of the crack, indicating the notch sensitivity of the material. It is interesting to point out that for specimen without pre-crack and under 8697 KPa confined pressure, microcracks start to develop approximately at 30% applied strain and the number of the microcracks increases significantly at 40% applied strain. Finally, the specimen fractures at 50% applied strain as a result of coalescence of microcracks and propagation of a dominant macrocrack. However, for the pre-cracked specimen, the crack starts to propagate, approximately, at 10% applied strain, which is in the linear region of the stress-strain curve, and no significant number of microcracks develop away from the crack tip. Experimental data indicate that in the immediate neighborhood of the crack tip, voids develop in the damage zone.
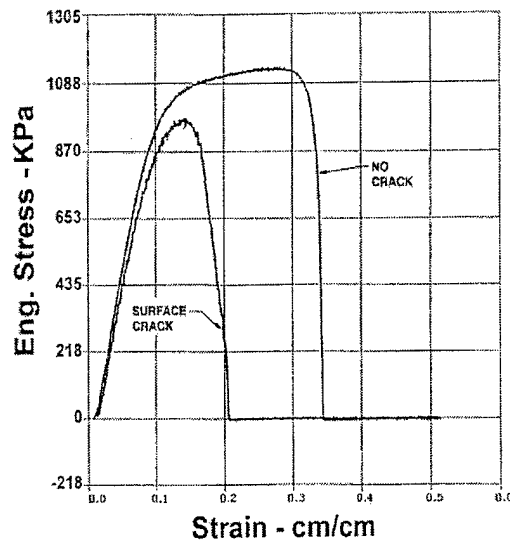

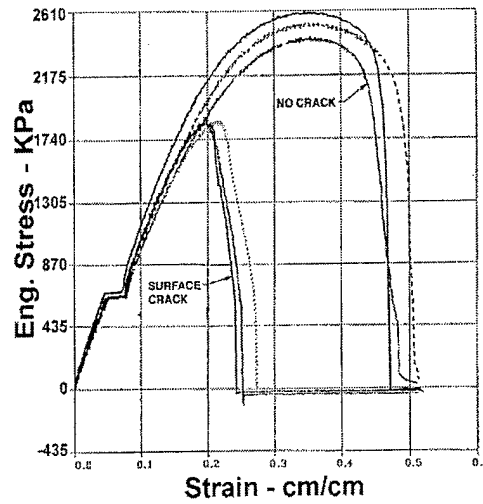Figure 2. Engineering stress versus strain (ambient pressure)

Figure 3. Engineering stress versus strain (8697Kpa pressure)

Typical crack tip profiles under ambient and 8697 KPa pressures are shown in Fig. 4. It is seen that the crack opening displacement (COD) under ambient pressure is larger than that under 8697 KPa pressure. Since the COD is related to the damage condition at the crack tip, the higher the damage the larger the COD, it is expected that the magnitude of the COD will decrease under the confined pressure condition as a result of the suppression of the damage. A similar behavior is observed when the distribution of the normal strain, ε_y, is plotted as a function of distance ahead of the crack tip, as shown in Fig.5. From Fig. 5, the normal strain is smaller under the 8697 KPa confined pressure condition.
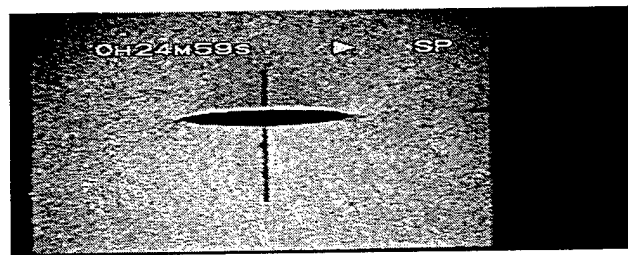
(a) 8697 KPa confined Pressure
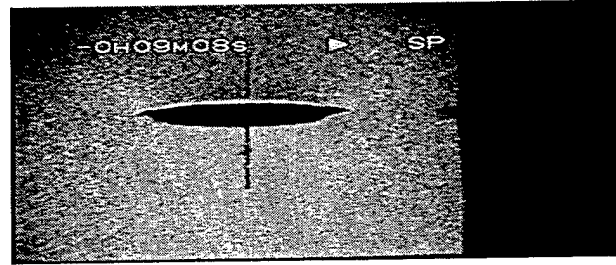
(b) Ambient Pressure

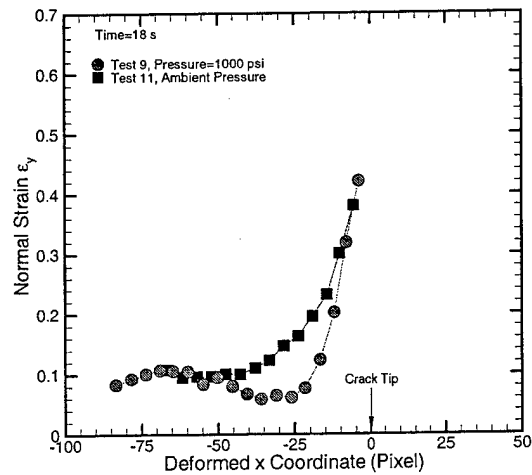Figure 4. Crack profiles under different confined pressure.

Figure 5. Normal strain distributions ahead of the crack tip

Typical plots of crack length, c, versus time, t, under different loading conditions are shown in Figs. 6 and 7. Under the ambient pressure and constant strain rate conditions, the crack grows with a relatively high velocity and the specimen fractures before the applied strain reaches 18% (Fig.6). However, in comparison to the ambient pressure condition, the higher confined pressure induces a delay in the onset of crack growth and a higher fracture strain. Figure 7 shows the crack length as a function of time under the constant strain condition. Under the constant strain condition, the crack continues to grow a short distance after the machine is stopped at the predetermined 18% strain level before it stops propagating. This kind of crack growth behavior is believed to be

related to the local stress at the crack tip and the viscoelastic nature of the material. When the specimen is under the constant strain condition, the stress will relax. However, the local stress at the crack tip may still be high enough to propagate the crack until the local stress at the crack tip is reduced to a threshold value below which no crack growth can occur. In addition, due to the material's viscoelastic nature, the local time-dependent material response lags behind and is not in phase with the applied deformation. The existence of a time scale or phase change between the applied load and the local response is a possible contributing factor responsible for the continued growth of the crack for a short distance after the machine is stopped.
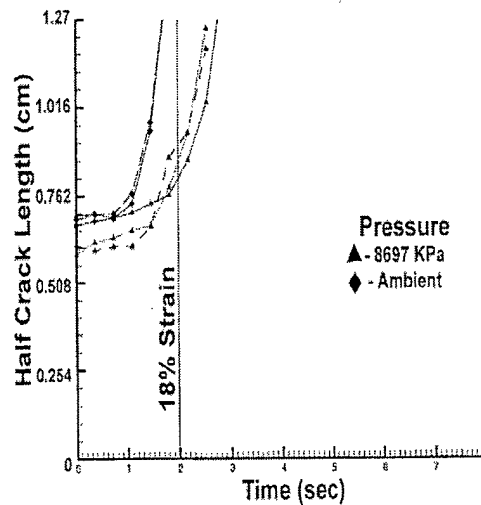

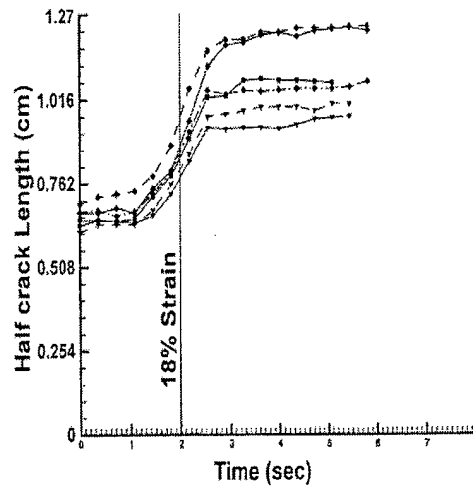Figure 6. Half crack length versus time (constant strain rate condition)

Figure 7. Half crack length versus time (constant strain condition).

A typical plot of crack growth rate versus time under the constant strain condition is shown in Fig. 8. According to Fig. 8, the crack growth rate continues to increase after the machine is stopped at 18% applied strain level and, then, decreases to zero velocity.
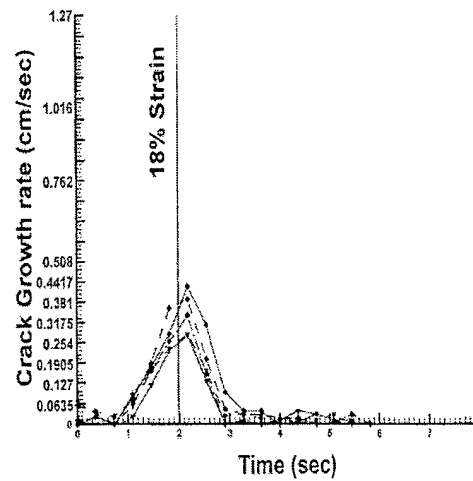

Figure 8. Crack growth rate versus time (constant strain condition)

Summary

In this study, the crack growth behavior in a particulate composite material under different loading conditions was investigated. Experimental findings reveal that the crack opening displacement and the normal strain ahead of the crack tip are smaller under 8697 KPa confined pressure than that under ambient pressure due to the suppression of damage under the high confined pressure condition. Experimental findings also indicate that, under the constant strain condition, the crack continues to grow a short distance after the machine is stopped at 18% applied strain level before it stops propagating.

References

[1] Beckwith, S.W. and Wang, D.T., "Crack Propagation in Double-Base Propellants," AIAA Paper 78-170, 1978.

[2] Liu, C.T., "Crack Growth Behavior in a Composite Propellant with Strain Gradients – Part II," Journal of Spacecraft and Rockets, 27, pp. 647-659,1990

[3] Liu, C.T. "Crack Propagation in a Composite Solid Propellant," Proceedings of the Society of Experimental Mechanics, Spring Conference, pp. 614-620,1990.

[4] Liu, C.T. and Smith, C.W., "Temperature and Rate Effects on Stable Crack Growth in a Particulate Composite Material," Experimental Mechanics, 36(3), pp. 290-295, 1996.

[5] Knauss, W.G., "Delayed Failure – The Griffith Problem for Linearly Viscoelastic Materials," International Journal of Fracture Mechanics, 6, pp.7-20, 1970.

[6] Schapery, R.A., On a Theory of Crack Growth in Viscoelastic Media, Report MM 2765-73-1, Texas A&M University, March 1973.

[7] Gonzalez, J., "Full Field Study of Strain Distribution Near the Crack Tip in Fracture of Solid propellant Via Large Deformation Digital Image Correlation and Optical Microscopy," Aeronautical Engineer Thesis, California Institute of technology, 1997.

[8] Vendroux, G. and Knauss, W. G., " Deformation Measurement at the Sub-Micron Size Scale: II. Refinements in the Algorithm for Digital Image Correlation," GALCIT SM Report 94-5, Apr. 1994.

[9] Sutton, M. A. Cheng, M., Peters, W. H., Chao, Y. J., and McNeill, S. R.," Application of an Optimized Digital Correlation Method to Planar Deformation Analysis," Experimental Mechanics, 4(3) 1986.